

Modeling of Plasma Assisted Combustion in Premixed Supersonic Gas Flow

Maxim A. Deminsky¹, Igor V. Kochetov², Anatoly P. Napartovich² and Sergey B. Leonov³

¹State Research Center RF “Kurchatov Institute”, Moscow, Russia

²State Research Center RF Troitsk Institute for Innovation and Thermonuclear Research (TRINITI), Troitsk, Moscow region, Russia

³Joint Institute for High Temperature RAS, Moscow, Russia

Abstract

A model for plasma assisted combustion of ethylene-air mixtures at conditions typical for scramjet combustion chamber is developed combining classical mechanisms of thermal combustion with non-thermal plasma chemistry. Numerical simulations showed that sufficiently strong reduction of ignition induction time at a reasonable energy cost can be realized with help of filamentary discharges. Starting from the discharge region, the gas mixture is heated due to exothermic reactions involving atomic oxygen and secondary chemical radicals. Temperature increment to the end of this stage for ethylene-air mixture is relatively small. An important effect of this stage is not heating but production of transient species. Then, a period with slow growth of temperature follows, which terminates by fast combustion. Processes causing the first fast growth of gas temperature are analyzed, and intermediate species controlling acceleration of ignition are determined numerically for plasma assisted combustion of stoichiometric mixture of ethylene with air. The value of the calculated induction time defined as a moment of the fast combustion is rather sensitive to the particular combustion mechanism adopted. This manifests a necessity to refine combustion mechanisms for conditions typical for scramjet combustion chamber with plasma initiation – one atmosphere pressure, static gas temperature around 700 K and appearance of atomic oxygen[†].

1. INTRODUCTION

Scramjet combustor is expected to provide propulsive energy for flights of hypersonic aircraft at an altitude of about 20 km with a Mach number M of about 8. Head wind is slowed down to $M \approx 2$ in the inlet on a system of attached shocks. Then it comes into combustor. As a result of slowing down, the static gas temperature rises to about 700 K and static gas pressure rises to about one atmosphere (see schematic of the scramjet engine in Fig. 1).

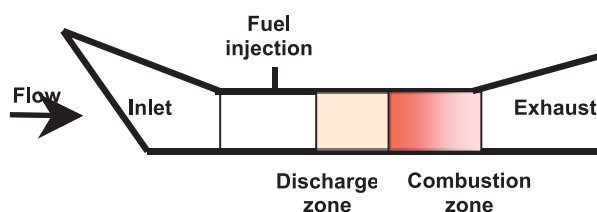


Figure 1. Simplified schematic of scramjet with uniform plasma induced ignition.

* kochet@triniti.ru

[†] Materials reported in this article were presented at Symposium “Chemical Physics of Low Temperature Plasmas” in honor of Prof M. Capitelli, on the occasion of his 70th birthday, Jan. 31- Feb. 1, 2011

The primary goal of designing a scramjet combustor is to decrease the combustion induction length below the length of combustion chamber. It is expected that use of non-thermal plasma may help to significantly accelerate ignition of air-fuel mixtures [1-4] at the expense of only moderate energy input.

Mechanisms of plasma induced combustion acceleration have been discussed in the literature: formation of atomic oxygen and other chemical radicals (see e.g., [5]; production of singlet delta oxygen molecules $O_2(a^1\Delta_g)$ [6-7]; chain ion-molecule reactions with radicals as intermediates [8]). Today, a majority of researchers believe that the main active species responsible for ethylene/air combustion acceleration is the atomic oxygen.

It was found in [5] that the most important source of atomic oxygen in plasma is dissociation of O_2 molecules in collisions with excited nitrogen molecules and by electron impact. Then oxygen atoms come into fast chemical reactions with hydrocarbons. Heat release in exothermic reactions results in fast gas-heating but the temperature increment is low. Afterwards, heating rate diminishes, and a plateau in temperature-time curve appears. The second step-wise growth of temperature with the delay determining the induction time is the fast mixture ignition resulting in the complete burning.

For description of the spontaneous ignition, a number of combustion mechanisms are known: GRI 3.0 [9], Konnov [10], UBC 2.0 [11], Kintech [12]. These mechanisms are verified for rather high initial gas temperatures (≥ 1100 K). At lower temperatures, the thermal production rate of chemical radicals is negligible. Radicals can be produced by natural sources (like cosmic rays) with rather low rate subject to strong fluctuations. As a result, the induction time (IT) in experiments cannot be controlled and leading to large variations in the observed induction times. Hence, no valid conclusion can be drawn from experiments about applicability of known combustion mechanisms at temperatures lower than about 1100 K. On the other hand, plasma activation of gas mixtures results in a large amount of chemical radicals. Then the role of spontaneous fluctuations of radicals is negligible, and the IT is a well defined function of active species amount. Adequacy of theoretical description of plasma assisted combustion depends on the accuracy of chemical reaction rate coefficients for the processes with chemical radicals involved. To verify plasma assisted combustion model for a specified fuel/oxidizer system one needs accurate experimental data on plasma initiated combustion for the system considered.

It is also known that at certain conditions the spontaneous ignition of hydrocarbons occurs over a few stages [13]. It manifests itself in the form of step-like growth of gas temperature separated by periods of slow growth. This phenomenon has received much attention in the recent years. The processes in "cold" and "blue" flames appearing in a course of oxidation and burning hydrocarbons and their derivatives in gas phase, have been reviewed in [14]. The emission of light observed in flames is mainly due to spontaneous emission from excited electronic states of molecules HCHO (in cold flames) and HCO (in blue flames). Particular attention has been paid to acetaldehyde (CH_3CHO) as a precursor of both cold and blue flames in Ref. [14].

Along with the appearance of multiple stages in fuel/air ignition, in some cases, the so-called *negative temperature coefficient* is observed experimentally (see e.g., [14]). It means that over a certain range of initial temperature, the IT actually increases with rise in initial temperature. In a recent paper [15] the combustion mechanism for *n*-butane was developed for a range of initial temperature between 530-900 K, which predicts that, for some conditions both two-stage burning and negative temperature coefficient exist.

It was shown in [3] that the minimum discharge energy input required for a successful ignition of stoichiometric C_2H_4 /air mixture under conditions representative of the scramjet combustor is impractically high. One of the ways to reduce the minimum ignition energy is usage of a filamentary discharge, allowing for utilization of heat and active species generated in chemical reactions in locations with high discharge power density for activation of gas molecules in the neighborhood. It was theoretically shown in [4] that usage of a filamentary discharge can significantly reduce the threshold specific energy input for ignition of ethylene/air mixture as compared with uniform discharge. The specific energy input (SIE) is defined as a ratio of the energy input to the fuel/air mixture mass flow rate.

The present paper aims to theoretically study in more detail, the processes influencing the formation of different stages, as well as their durations in plasma assisted ignition for conditions representative of the scramjet combustor. The different processes controlling the rate of gas heating are investigated for

stoichiometric mixtures of H_2 /air and C_2H_4 /air. The intermediates that the strongest influence on the IT period are identified with respect to various mechanisms of the spontaneous ignition.

2. SELF-CONSISTENT MODELING OF PLASMA ASSISTED COMBUSTION IN SUPERSONIC FLOW

The complexity of plasma description, in particular at high pressures is associated with two factors: (1) a large number of reactions taking place in the plasma, which are very specific for a given gas composition; (2) a non-uniformity of plasma in a majority of discharge types. Evidently, taking into account both of these points presents a formidable problem. A traditional approach to modeling realistic plasma devices consists of two phases. In the first step, the plasma is considered to be in-plane uniform, and its transportation with gas flow is taken into account (so-called plug-flow model). In this step, major attention is paid to a correct description of electron kinetics and reactions of excited particles and chemical radicals.

The model incorporates kinetic equations for reaction steps involving charged and neutral species including electrons, positive and negative ions, molecules, excited species, and radicals. The efficiency of production of the chemically active species is determined by an electron energy distribution function (EEDF) formed by electric field and collisions with atoms and molecules. The EEDF is found numerically by solving the electron Boltzmann equation (BE) in two-term approximation. In the Boltzmann equation, all processes of inelastic scattering by atoms and molecules, including excitation of rotational levels and molecular vibrations, excitation of electronic levels, dissociation, ionization and electron attachment processes in electron-molecule collisions are taken into account.

The influence of physical parameters such as gas temperature, pressure, and applied electric field on the EEDF shape can be described adequately by one combined parameter controlling practically all important discharge characteristics. This is the value of the reduced electric field strength E/N , where E is the electric field strength and N is the total gas number density. Besides, change in chemical composition of the gas is also an important factor. The variation of electric field strength is controlled by electric circuit parameters. For the steady state regime, the E/N parameter and gas composition change along the flow. The solution BE was obtained whenever needed; i.e., whenever the key parameters (E/N and mixture composition) changed by a certain value.

The set of balance equations for charged plasma species (including positive and negative ions, electrons) is solved jointly with the continuity equations for neutral species, which include not only the reactants but also the products of plasma chemical processes. The change in temperature and gas composition along the flow induced by the discharge and chemical reactions should be taken into account. The chemically reactive gas flow in the variable-area duct is described in frames of a pseudo-one-dimensional approximation:

$$\frac{dp}{dx} + \rho u \frac{du}{dx} = 0, \quad (1)$$

$$\rho u \frac{d}{dx} \left(h + \frac{1}{2} u^2 \right) = jE, \quad (2)$$

$$\rho u S = \dot{Q}, \quad (3)$$

$$\frac{d\gamma_i}{dx} = F_i(p, T, \gamma_1, \gamma_2, \gamma_3, \dots, \gamma_N, j, E). \quad (4)$$

Here p and ρ are gas pressure and mass density, respectively; u gas flow velocity; h specific enthalpy; j electric current density; E electric field strength; S is the duct section area; \dot{Q} is mass flow-rate of gas;

$\gamma_i = \frac{n_i}{\mu \sum_i n_i}$ is the fractional concentration of i -th component divided by the average molar weight (n_i is the number density of i -th component, $\mu = \sum_i \mu_i Y_i$, μ_i is molar weight of i -th component, $Y_i = \frac{n_i}{\sum_i n_i}$ is the mole fraction); $F_i(p, T, \gamma_1, \gamma_2, \gamma_3, \dots, \gamma_N, j, E)$ is the mass production rate in i -th reaction; T is the static gas temperature. An energy loss by spontaneous emission is neglected in eqn. (2). The system of equations (1-4) is closed by the state equation and an expression for the specific enthalpy of the gas mixture:

$$p = \frac{R\rho T}{\mu}, \quad (5)$$

$$h = \sum_i H_i(T) \gamma_i. \quad (6)$$

Here R is the universal gas constant; $H_i(T)$ is the molar enthalpy of i -th component.

Equations (1)-(4) were solved in parallel with a system of kinetic equations for charged particles (electrons, positive and negative ions) and with the electric circuit equation. The electric circuit comprises a capacitor and a ballast resistor. The electric circuit equation was taken in the form:

$$(R_b + R_{DISCH}(t)) \frac{dq}{dt} + \frac{q}{C} = 0. \quad (7)$$

Here q is electric charge on the discharge capacitor C , R_b , $R_{DISCH}(t)$ are the ballast and discharge resistance, respectively. Two cases were analyzed: the short pulse discharge and DC glow discharge in gas flow. In the first case, the values of the charge capacity and of the initial voltage U_0 were found from the condition that the pulse duration and input energy are equal to their prescribed values. In the second case, the capacity was taken large enough to neglect variation of the charge on the capacity during the gas residence time within the discharge region.

The self-consistent electron scattering cross section sets were taken from refs. [16-18] for N_2 , O_2 and C_2H_4 molecules, respectively. Kinetic scheme and rate coefficients for reactions of excited molecules and for ion-molecular reactions in air are taken from ref. [16]. Rate coefficients for reactions of excited nitrogen molecules with ethylene are taken from ref. [19].

The model for plasma assisted combustion of hydrogen/dry air mixture described in Ref. [5] contains 25 chemical reactions. In the model for ethylene combustion in air [3], the number of reactions between neutral components is equal to 294. The Chemical Workbench software program [20] was used to construct the thermal chemistry block of the model.

To give an idea about order of magnitude of effects in plasma assisted combustion, the electron energy balance found by solution of the BE is presented in Fig. 2 as a function of E/N for the stoichiometric C_2H_4 /air mixture. For clarity, only three channels are shown, most important for ignition initiation: 1) electron energy loss to fast heating (elastic collisions and excitation of molecular rotations), 2) vibrational excitation leading to delayed gas heating, and 3) losses to dissociation of O_2 and C_2H_4 molecules. The following elementary processes of O_2 dissociation were taken into account: two channels for electron impact dissociation with $2O$ and $O+O(^1D)$ as products; dissociation in collisions with electronic excited N_2 molecules [19]. The cross section for C_2H_4 electron impact dissociation was taken from [18] as for a process with the threshold 4.6 eV and products C_2H_3+H . The rate coefficient for quenching of $N_2(A^3\Sigma_u^+)$ by C_2H_4 is equal to $1.1 \cdot 10^{-10} \text{ cm}^3/\text{s}$ [19]. We have assumed that the main channel for this process is dissociation of C_2H_4 onto C_2H_3+H . Information about

quenching of higher electronic states of N_2 by C_2H_4 is not available. We take the same rate coefficient and same products as for quenching of $N_2(A^3\Sigma_u^+)$.

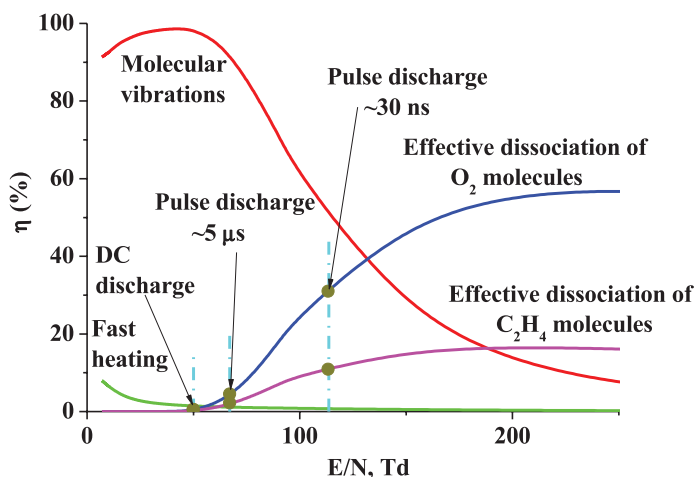


Figure 2. Electron energy partitioning in stoichiometric mixture of C_2H_4 with dry air as a function of E/N . The vertical lines show the typical E/N values for different types of discharge in the CH_4 -air mixture.

Values of E/N parameter, typical for steady state and pulsed discharges of different duration, are indicated in Fig. 2 by chain vertical lines. It is seen that dissociation efficiency for steady state discharges are much lower than for pulsed discharges. The shorter discharge pulse, the greater is dissociation efficiency of a discharge.

Results of numerical simulations for a constant-area duct are shown in Fig. 3 for stoichiometric H_2 /air mixture ignited by the DC glow discharge with variable SEI regulated by variation in the discharge region length. The entrance to the discharge region is located at $X=0$. The flame front exhibits itself as a rapid fall in the Mach number and simultaneous increase in static temperature.

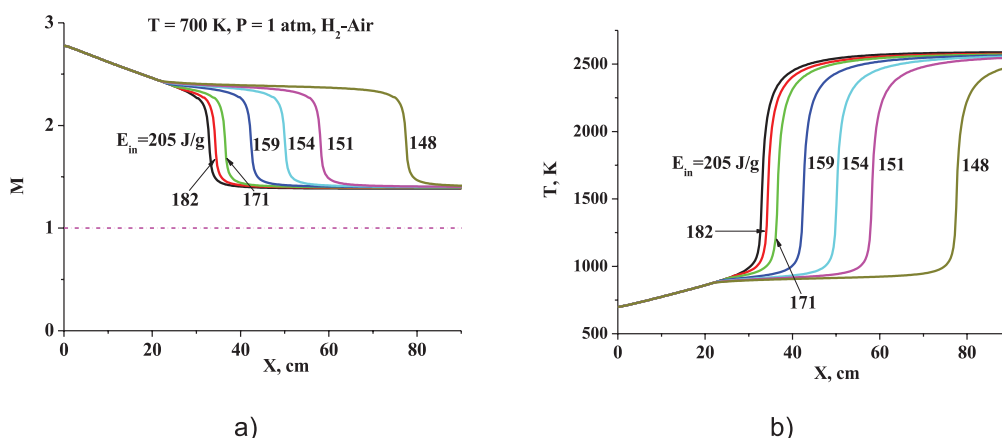


Figure 3. Mach number (a) and static temperature (b) variation along the flow for gas mixture H_2 /air at different discharge energy inputs. The SEI grows for curves in direction from the right to the left.

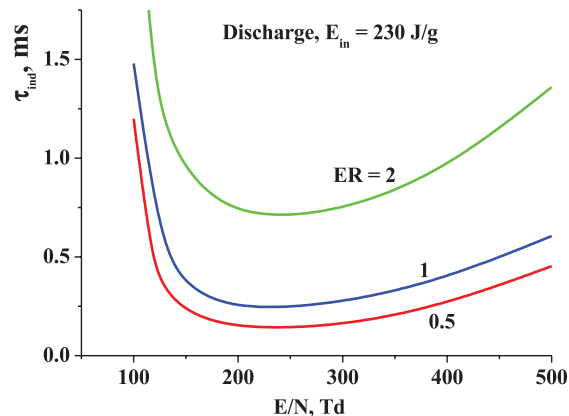


Figure 4. Induction time as a function of E/N for various mixtures C_2H_4 - air. $T_0=700$ K, $P_0=1$ atm.

It was shown earlier [21] that for supersonic flow in scramjet combustor an additional simplification by setting gas number density constant along the flow introduced quite a small error in the calculated induction time (IT) in comparison with solving a full system of equations for gas-dynamic flow. In this work, the most results of further numerical simulations are found by implementing the plug-flow model with fixed gas number density.

As shown in [3], the typical SEI required for plasma initiation of the C_2H_4 /air mixtures is about 230 J/g. At this level of the SEI, the discharge initiated IT is a function of E/N and the equivalence ratio (ER). To illustrate these correlations, the simplified version of the electric discharge model was employed. In this version, the E/N parameter was kept constant until the energy input in the discharge achieves the assigned value (230 J/g) and then turned to zero.

Fig. 4 shows the IT as a function of E/N parameter at three values of ER. There exists a minimum in IT values at E/N in the interval (220-250) Td. The IT grows with the ER varied from 0.5 to 2. Fig. 5 compares spontaneous IT and plasma initiated IT as functions of ER. For comparison purposes, the initial temperature for thermal initiation is taken of the magnitude, which provides the IT values of the same level as for plasma initiation with the SEI=230 J/g and $E/N=200$ Td. It is clearly seen from Fig. 5 that the IT values are of the same magnitude at the thermal enthalpy density increment more than twice of the discharge SEI. Dependence of the IT on the ER is similar for thermal and discharge initiation, except the limit of lean mixtures.

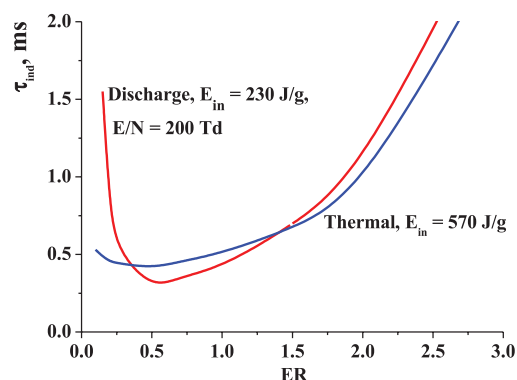


Figure 5. Induction time as a function of equivalence ratio for discharge and thermal initiation.

No experimental data exist about plasma assisted combustion of premixed ethylene/air mixtures for conditions of the scramjet combustor. Therefore, our kinetic model was verified by comparison with experimental data [22-23] for plasma assisted combustion in subsonic flow at room gas temperature and pressure of a few tens of Torr. It was shown in [24] that our model provides reasonably good agreement with experimental data [22-23] on gas heating rate, the threshold energy input and time evolution of atomic oxygen.

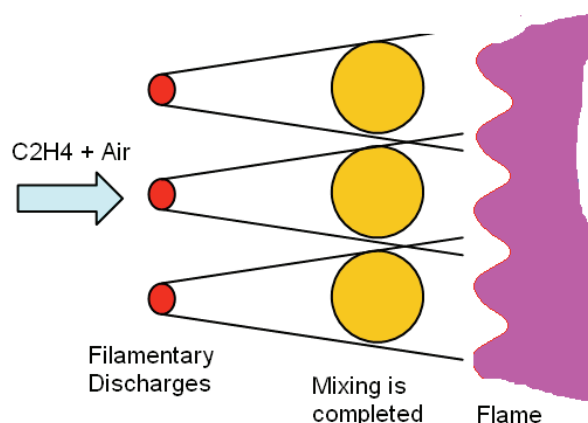


Figure 6. Sketch of supposed filamentary discharge (view from above).

It was reported in [25] that usage of filamentary discharges can essentially speed-up ignition of C_2H_4 /air mixture at low energy cost. Fig. 6 shows schematically the periodic system of transverse pulsed micro-discharges under consideration. They can be realized with a special electrode system. It is of great interest to simulate numerically such a system using various approximations for description of gas dynamic flow. Since typical duration of a pulse discharge at atmospheric pressure is short in comparison with gas dynamic processes the pulse discharge occupies a fixed volume V_0 . Then the activated gas mixture is expanded and mixed continuously with the unexcited mixture. As the unexcited mixture is at a lower temperature, this mixing leads to reduction in temperature. However, fast exothermic reactions induced by the discharge may compensate gas cooling associated with mixing. The detailed modeling of a system of intermixing streams is a rather complicated task, taking into account necessity to describe correctly combustion chemistry. To evaluate ignition efficiency in conditions of non-uniform excitation, a model of distributed mixing within a finite length was formulated, the numerical code was modified, and numerical simulations were performed for ignition of supersonic C_2H_4 /dry-air mixture by the system of transverse discharges. Calculations were made for the premixed stoichiometric mixture at the static pressure 1 bar and static gas temperature 700 K.

The process of distributed mixing of activated and passive plane jets is characterized by two parameters: 1) ratio of the volume occupied by jets at complete mixing to the volume of discharge filaments, V/V_0 ; 2) time of mixing, Δt_{mix} , which is controlled by a period of filaments and expansion rate of mixed gas stream area. Calculations were performed at these variable parameters in order to find the optimum conditions with respect to discharge energy required to have $IT=300 \mu s$. Due to limitations on the filament radius put by constriction phenomena, it is reasonable to take the parameter V/V_0 as large as possible. In general, mixing of two adjacent layers proceeds through symmetric expansion of mixed layer to both sides. If the activated layer is notably thinner than the passive layer, at a short distance it disappears, being absorbed by the mixed layer.

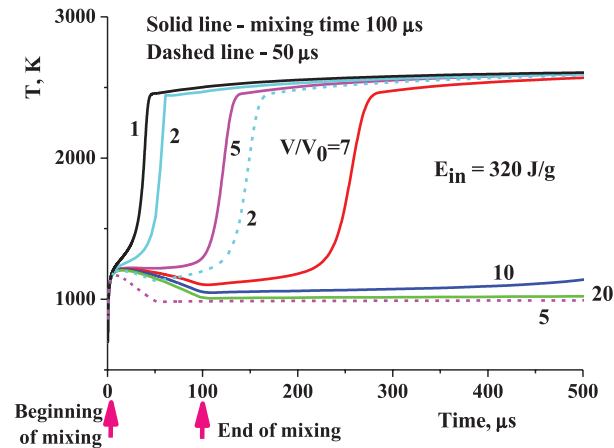


Figure 7. Predicted gas temperature evolution for various mixing times and dilution coefficients. Stoichiometric C_2H_4 -air mixture. $P_0 = 1$ atm, $T = 700$ K, $M = 2.6$.

Fig. 7 demonstrates evolution of static gas temperature in mixed layer at variable V/V_0 parameter for two values of mixing time. The mixing time value exerts very strong influence on temperature evolution. At shorter mixing time $50 \mu s$, no ignition is observed for reasonable time at $V/V_0 > 2$, while at $\Delta t_{mix} = 100 \mu s$ the IT is about $300 \mu s$ at $V/V_0 = 7$. Sensitivity of the IT to the value of mixing time is explained by competition of gas cooling due to mixing and gas heating in the exothermic reactions.

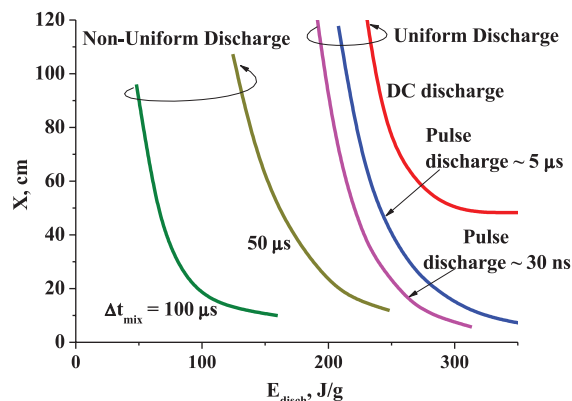


Figure 8. Ignition lengths for uniform and non-uniform discharge initiations. Stoichiometric C_2H_4 -air mixture. $P_0 = 1$ atm, $T = 700$ K.

Fig. 8 summarizes results of numerical simulations for plasma assisted ignition of C_2H_4 /dry-air mixture for conditions of the scramjet combustor. Usage of pulse periodic plasma allows one to get higher ignition efficiency. For shorter discharges the IT is shorter. However, it is a problem of practical realization of discharge of such type. Usage of a system of micro-discharges (filaments) allows one to significantly increase the efficiency of plasma assisted combustion approach for scramjet combustor.

3. INFLUENCE OF INTERMEDIATES ON INDUCTION TIME VALUE

As the next step in analyzing roles played by various byproducts, calculations were performed with help of our numerical model of plasma assisted combustion. The Chemical Workbench software [20] was used for numerical simulations of plasma assisted combustion for conditions of scramjet

combustor. This package allows us to integrate a system of kinetic equations for neutral chemical species and charged particles together with gas temperature found from thermal balance equation. The Kintech mechanism was employed for thermal chemistry description [12].

We use the simplified approach to modeling pulse discharge. The electric field strength was set as a constant within some time interval, which was varied to change the SEI. Calculated evolution of gas temperature of stoichiometric ethylene/air mixture subjected to pulse discharge at $E/N=200$ Td with $SEI = 225$ J/g is shown in Fig. 9 (“base” curve). The first vertical arrow indicates the discharge duration. During the discharge, gas is heated in vibrational relaxation processes and in dissociation processes due to energy defect released both, in direct electron impact and in collisions with electronic excited molecules. After discharge pulse termination, gas is heated predominantly in exothermic reactions involving oxygen atoms and secondary species.

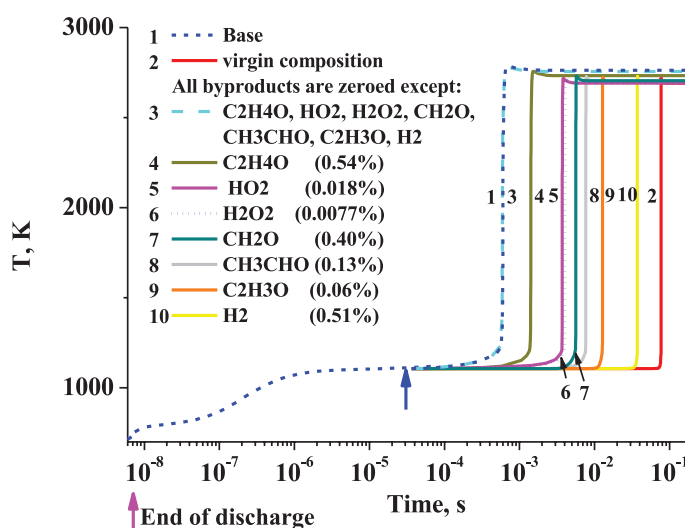


Figure 9. Calculated temperature evolution at pulse discharge initiation of stoichiometric C_2H_4 -air mixture with diagnostic change of gas composition at the moment shown by the blue arrow. The initial static temperature 700 K, pressure 1 atm, $E/N=200$ Td, $E_{in}=225$ J/g.

To get deeper insight into chemical mechanisms operating in afterglow stage, the following procedure was developed. At the selected moment of activated mixture evolution, which is shown in Fig. 9 by the second arrow (37 μ s), calculations were stopped; the gas mixture composition was changed in a prescribed manner and then calculations were continued with new initial conditions. Concentrations of intermediates at the stop moment are indicated in the legend in Fig. 9. The “virgin” curve shows evolution of gas temperature when the initial gas composition was restored. In this case, the IT is the longest one and corresponds to the spontaneous ignition at initial temperature equal to its current value at the moment when the procedure is switched on. The “base” curve corresponds to the “non-stop” calculations. It is found that the IT does not change with respect to the “base” case when keeping unchanged concentrations of the following species: C_2H_4O (vinyl alcohol), HO_2 , H_2O_2 , CH_2O , CH_3CHO (acetaldehyde), C_2H_3O , and H_2 . Further calculations with turning to zero concentrations of all intermediates except the selected one demonstrate that the above sequence of species is ordered by reduction of their influence on the IT value (numbers 4-10 in Fig. 9). It means that the most important species is vinyl alcohol (C_2H_4O , $C=C-OH$).

4. INDUCTION TIME PREDICTIONS WITH DIFFERENT COMBUSTION MECHANISMS

It was shown in [5] that atomic oxygen is the most important chemical agent produced in the discharges. To separate plasma and chemical effects, it is convenient to analyze roles of various chemical intermediates at addition of oxygen atoms into the premixed C_2H_4 /dry-air mixture. Then purely chemical codes with various combustion mechanisms can be employed. This analysis was made with usage of three combustion mechanisms: GRI Mech 3.0, Konnov and Kintech.

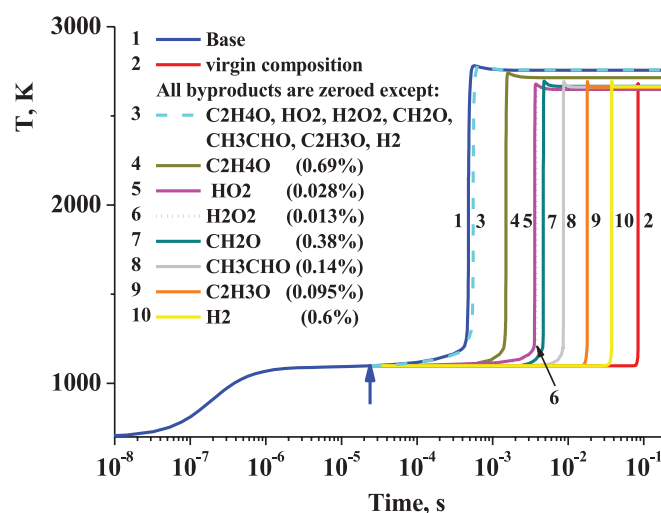


Figure 10. Calculated temperature evolution at ignition induced by O atoms for stoichiometric C_2H_4 -air mixture with diagnostic change of gas composition at the moment shown by the blue arrow. The initial static temperature 700 K, pressure 1 atm, 1.9% O.

The initial O-atom concentration for every combustion mechanism was fit to get the induction time value of the order of a few hundreds of μs . Fig. 10 shows results of numerical simulations for the Kintech mechanism at O concentration added 1.9% and the moment selected for gas composition change is about 23 μs . Concentrations of intermediate species at this moment are indicated in the legend in Fig. 10. Designations are the same as in Fig. 9. As expected, results of the analysis for discharge and O-atom initiations are in close agreement. The same sequence of the intermediates ordered by their impact on the ignition delay is predicted in both cases.

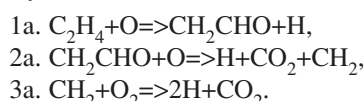
The similar calculations were performed for analyzing O-atom induced ignition of stoichiometric C_2H_4 /dry-air mixture using GRI Mech 3.0 and Konnov mechanisms. The list of intermediate species HO_2 , H_2O_2 , CH_2O , C_2H_3O , required to have the IT value equal to that in the “base” case, is the same for both mechanisms. The number one species in the Kintech mechanism, C_2H_4O , was not recognized as one influencing on the IT in frames of GRI Mech 3.0 and Konnov mechanisms. Actually, in the last both mechanisms there is no effective reaction pathway leading to ethenol formation at conditions under consideration.

The specific feature of the Kintech mechanism for ethylene oxidation is existence of reactions sequences named as “low temperature branch”, which are not present in the classical GRI Mech mechanism. Actually, these reactions sequences per se are included in the Konnov mechanism. In the Kintech mechanism, rate constants of respective additional reactions were independently checked. The analysis was based on recent compilation [26] of experimental rate constants of reactions important in combustion chemistry. Besides, most recent experimental and theoretical data, general physical and chemical laws (spin conservation, orders of magnitude of pre-exponential factors), and thermochemical data were used in the analysis. As a result, reaction mechanism was composed and includes

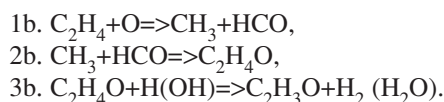
444 reversible reactions and 86 species. The description of the Kintech mechanism in more detail can be found in ref. [12].

It is noteworthy that despite the scatter in induction time values calculated by different combustion mechanisms, time evolution of gas temperature induced by addition of O-atoms has common specific features: appearance of two stages with the first fast growth followed by the plateau and then the second fast large step.

The two-stage temperature evolution originates from the complicate kinetics of the oxidation process. Kinetic analysis indicates that at the early post discharge phase the oxidation is chain branched process with accumulation of the intermediate active species like C_2H_4O , CH_2CHO ($2H=C^*-C=O$). In particular, in discharge and afterglow phases oxidation proceeds in reactions of ethylene with atomic oxygen followed by fast radical reactions at the time scale up to $\sim 10^{-6}$ s:

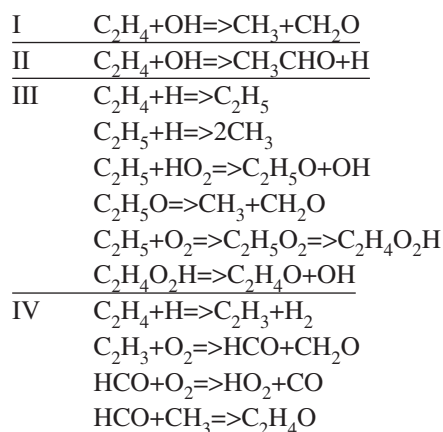


This mechanism has chain character with degree of the branching higher than 1. Another important pathway is formation of C_2H_4O with followed slow transformation to C_2H_3O ($C=C-O^*$, vinyloxy radical):



These reactions lead to termination the chain with formation of relatively long-lived products. The ratio the rates of the radical regeneration (1a) and of formation of relatively "stable" product, C_2H_4O , (1b) is about 2.6 at energy input 240 J/g, at the static gas temperature $T=700$ K, pressure $P=1$ atm.

The plateau is characterized by a high concentration of intermediates formed in numerous reactions between radicals. On this stage, concentrations of the active species are stabilized. In particular, bimolecular reactions involving active species become comparable with chain propagation reaction rates in their influence on the active species losses. Finally, at this stage the type of the chain processes changes from branched to degenerated type, when one radical reproduces only one new radical in overall chain reaction. A plenty of chemical reactions at plateau, which are important for evolution of the gas composition prior to ignition, can be ordered into four pathways (I-IV).



The branching ratio between the pathways is I:II:III:IV $\sim 1:2:1:2$ at the energy input 240 J/g, initial gas temperature $T=700$ K, pressure $P=1$ atm. These reactions lead to formation on the plateau of such intermediates as C_2H_4O , C_2H_5O , HCO , CH_2O , CH_3CHO , H_2O_2 .

5. GAS HEATING IN CHEMICAL REACTIONS

In order to get better insight into nature of plasma induced two-stage ignition we have analyzed in more detail processes controlling gas heating rate within the transient periods.

5.1. Hydrogen combustion

We start the analysis from the simplest system of stoichiometric hydrogen/dry-air mixture with added O atoms in the amount 0.32% using the combustion mechanism described in detail in [5]. To get an insight into chemical mechanisms of the first step in gas temperature growth, let us analyze individual inputs of specific reactions into the gas heating process. The reactions exerting influence on gas heating rate are listed in Table 1 in the descending order. It is seen that the only reaction of O atoms with molecules is #11 in Table 1. At these conditions, formation of ozone is too slow and can be neglected.

Table 1. List of reactions giving largest input into gas heating rate for the mixture H₂/air (conditions of Fig. 11, moment 20 μs)

| No | Reaction |
|----|--|
| 1 | $\text{H} + \text{HO}_2 \rightleftharpoons \text{OH} + \text{OH}$ |
| 2 | $\text{OH} + \text{H}_2 \rightleftharpoons \text{H} + \text{H}_2\text{O}$ |
| 3 | $\text{H} + \text{O}_2 + \text{N}_2 \Rightarrow \text{HO}_2 + \text{N}_2$ |
| 4 | $\text{H} + \text{O}_2 + \text{H}_2 \Rightarrow \text{HO}_2 + \text{H}_2$ |
| 5 | $\text{O} + \text{HO}_2 \rightleftharpoons \text{OH} + \text{O}_2$ |
| 6 | $\text{H} + \text{HO}_2 \rightleftharpoons \text{H}_2 + \text{O}_2$ |
| 7 | $\text{O} + \text{OH} \rightleftharpoons \text{H} + \text{O}_2$ |
| 8 | $\text{OH} + \text{HO}_2 \rightleftharpoons \text{H}_2\text{O} + \text{O}_2$ |
| 9 | $\text{H} + \text{O}_2 + \text{O}_2 \Rightarrow \text{HO}_2 + \text{O}_2$ |
| 10 | $\text{H} + \text{OH} + \text{M} \Rightarrow \text{H}_2\text{O} + \text{M}$ |
| 11 | $\text{O} + \text{H}_2 \rightleftharpoons \text{OH} + \text{H}$ |

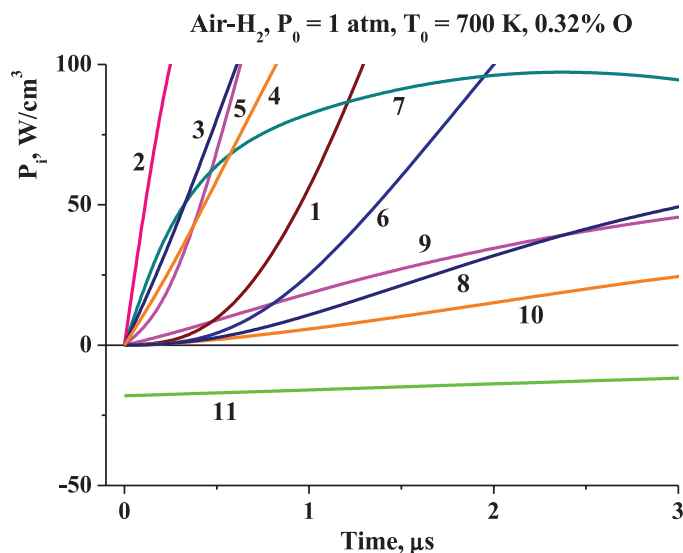


Figure 11. Heat release rate in a short-time limit in reactions listed in Table 1. O-atom induced ignition of stoichiometric H₂-air mixture.

This reaction is endothermic one. However, the products in this reaction are high-reactive radicals H and OH, which participate in fast exothermic reactions (2-4, 9, 10). In reactions 3, 4, and 9 one more high-reactive radical HO_2 is formed, which is involved in exothermic reactions 1, 5, 6, and 8. The heating rates in secondary exothermic reactions approach maxima at times around 10 μs , then diminish due to recombination of radicals. To clarify the role of gas cooling in primary reaction 11, Fig. 11 shows gas heating (cooling) rates in processes (1-11) at short times. It is seen that gas cooling effect in reaction 11 is compensated by heat release in secondary reactions on time scale about 100 ns.

5.2. Ethylene combustion

It is instructive to analyze in detail mechanisms of gas heating on earlier stage of ethylene ignition induced by O-atoms with concentration 1.4%. This study was performed with help of our numerical code described in [3]. Reactions giving the largest input into the gas heating rate at the time moment 2 μs are listed in Table 2 in the descending order. Time evolution of heat release rates in the specified reactions is shown in Fig. 12. The secondary reactions (1, 3-10) give a comparable input into heat release rate with maxima around 100 ns. This interval is much shorter than the delay in maximum formation in the heating rate for H_2/air stoichiometric mixture (about 10 μs). Evolution of concentrations of species involved in reactions listed in Table 2 is shown in Fig. 13. O atom concentration falls down within about 0.5 μs . There are long-lived radicals CH_2O , HO_2 , CH_3 evolution of which proceeds on a scale of microseconds.

Table 2. List of reactions giving largest input into gas heating rate for the mixture $\text{C}_2\text{H}_4/\text{air}$ (conditions of Figs. 12, 13, moment 2 μs)

| No | Reaction |
|----|---|
| 1 | $\text{HCO} + \text{O}_2 \rightleftharpoons \text{HO}_2 + \text{CO}$ |
| 2 | $\text{O} + \text{C}_2\text{H}_4 \rightleftharpoons \text{CH}_3 + \text{HCO}$ |
| 3 | $\text{H} + \text{CH}_3 + \text{M} \rightleftharpoons \text{CH}_4 + \text{M}$ |
| 4 | $\text{O} + \text{CH}_3 \rightleftharpoons \text{H} + \text{CH}_2\text{O}$ |
| 5 | $\text{H} + \text{HO}_2 \rightleftharpoons \text{OH} + \text{OH}$ |
| 6 | $\text{O} + \text{CH}_3 \rightleftharpoons \text{H} + \text{H}_2 + \text{CO}$ |
| 7 | $\text{O} + \text{CH}_2\text{CHO} \rightleftharpoons \text{H} + \text{CH}_2 + \text{HCO}_2$ |
| 8 | $\text{O} + \text{HCO} \rightleftharpoons \text{H} + \text{CO}_2$ |
| 9 | $\text{O} + \text{CH}_2 \rightleftharpoons \text{H} + \text{HCO}$ |
| 10 | $\text{O} + \text{HCO} \rightleftharpoons \text{OH} + \text{CO}$ |
| 11 | $\text{O} + \text{C}_2\text{H}_4 \rightleftharpoons \text{H} + \text{CH}_2\text{CHO}$ |

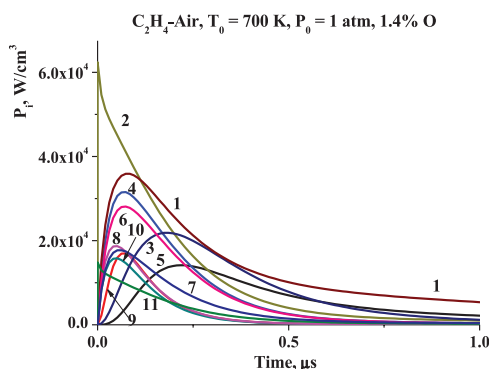


Figure 12. Heat release rate in reactions listed in Table 2 for O-atom initiation. Stoichiometric C_2H_4 -air mixture.

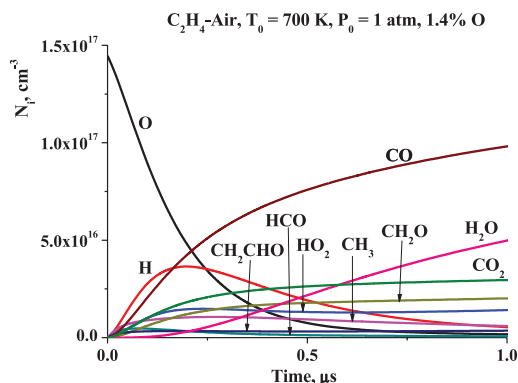


Figure 13. Calculated evolution of some components at initiation by O atoms. Stoichiometric C_2H_4 -air mixture.

6. CONCLUSION

Numerical modeling of plasma or O-atom assisted ignition of hydrogen and hydrocarbons premixed with dry air demonstrates appearance of two step-wise changes in evolution of gas temperature. At the first stage O atoms and other radicals produced by a discharge convert into some intermediate species. Chemical reactions on this stage are, as a rule, exothermic resulting in a fast gas heating, which is practically stopped at some level. Chemical reactions possessing high heat release rates are identified for hydrogen/air and ethylene/air mixtures. The second stage corresponds to complete burning of a fuel. Evolution to the final ignition has a form of rather slow growth of gas temperature (plateau). In this interval, chemical reactions take place between intermediate species. For ethylene/air mixture the most important intermediates strongly affecting on the induction time are the following: $\text{C}_2\text{H}_4\text{O}$, HO_2 , and H_2O_2 (Kintech mechanism); HO_2 , H_2O_2 and CH_2O (GRI Mech 3.0 and Konnov). Various combustion mechanisms predict different roles played by these species in the ignition.

The large scatter in values of induction time for plasma induced ignition predicted with different combustion mechanisms is convincing argument for necessity of further improvement of combustion mechanism for conditions typical for scramjet combustors: static gas pressure 1 atm., temperature 700 K.

REFERENCES

- [1] Leonov S., Bityurin V., Bocharov A. et al., Hydrocarbon fuel ignition in separation zone of high speed duct by discharge plasma. *Proc. 4th Workshop "PA and MHD in Aerospace Applications"*. M: IVTAN, 2002.
- [2] Starikovskaia S.M., Plasma assisted ignition and combustion, *J. Phys. D: Appl. Phys.* 2006, 39, R265-R299.
- [3] Kochetov I.V., Leonov S.B., Napartovich A.P., Plasma ignition of combustion in a supersonic flow of fuel-air mixtures: Simulation problems, *High Energy Chemistry*, 2006, 40, 98-104.
- [4] Napartovich A.P., Kochetov I.V., Leonov S.B., Numerical simulation of ignition pre-mixed ethylene-air mixture by system of microdischarge, *Teplofiz. Vys. Temp.*, 2010, 48, 60-66.
- [5] Napartovich A.P., Kochetov I.V., Leonov S.B., Calculation of the dynamics of ignition of an air-hydrogen mixture by nonequilibrium discharge in a high-velocity flow, *High Temperature*, 2005, 43, 673-679.
- [6] Starik A.M., Kozlov V.E., Titova N.S., On the influence of singlet oxygen molecules on the speed of flame propagation in methane-air mixture, *Combustion and Flame*, 2010, 157, 313-327.
- [7] Popov N.A., The effect of nonequilibrium excitation on the ignition of hydrogen-oxygen mixtures, *High Temperature*, 2007, 45, 261-279.
- [8] Starik A.M., Titova N.S., Kinetics of ion formation in the volumetric reaction of methane with air, *Combustion, Explosion, and Shock Waves*, 2002, 38, 253-268.

- [9] Smith G.P., Golden D.M., Frenklach M., et al, GRI Mech 3.0, 1999. (http://www.me.berkeley.edu/gri_mech/).
- [10] Konnov A.A. Detailed reaction mechanism for small hydrocarbons combustion. Release 0.5, 2000. (<http://homepages.vub.ac.be/~akonnov/>).
- [11] Huang J. and Bushe W.K., Experimental and kinetic study of autoignition in methane/ethane/air and methane/propane/air mixtures under engine-relevant conditions, *Combustion and Flame*, 2006, 144, 74-88. (<http://kbspc.mech.ubc.ca/kinetics.html>).
- [12] KINTECH. Kinetic technologies. Chemical Workbench (<http://www.kintech.ru>).
- [13] Sokolik A.S., Self-ignition and combustion in gases, *Usp. Fiz. Nauk.*, 1940, 23, 209-250.
- [14] Basevich V.Ya., Frolov S.M., Kinetics of “Blue” flames in the gas-phase oxidation and combustion of hydrocarbons and their derivatives, *Usp. Khim.*, 2007, 76, 927-944.
- [15] Strelkova M.I., Safonov, A.A. Sukhanov L.P. et al, Low temperature n-butane oxidation skeletal mechanism, based on multilevel approach, *Combustion and Flame*, 2010, 157, 641-652.
- [16] Akishev Y.S., Deryugin A.A., Karalnik V.B., et. al., Numerical simulation and experimental study of an atmospheric-pressure direct-current glow discharge, *Plasma Phys. Rep.*, 1994, 20, 511-524.
- [17] Ionin A.A., Kochetov I.V., Napartovich A.P., Yuryshv N.N., Physics and engineering of singlet delta oxygen production in low-temperature plasma, *J. Phys. D: Appl. Phys.*, 2007, 40, R25-R61.
- [18] Hayashi M., Electron collision cross sections determined from beam and swarm data by Boltzmann analysis in “Nonequilibrium Processes in Partially Ionized Gases” Eds. M. Capitelli and J. N. Bardsley, *NATO ASI Series B: Physics* v. 1990, 220, 333-340, Plenum Press, N-Y.
- [19] Herron J.T., Evaluated chemical kinetics data for reactions of $N(^2D)$, $N(^2P)$, and $N_2(A^3\Sigma_u^+)$ in the Gas Phase, *J. Phys. Chem. Ref. Data*, 1999, 28, 1453-1483.
- [20] Deminsky M., Chorkov V., Belov G., et al, Chemical Workbench - Integrated Environment for Materials Science, *Computational Materials Science*, 2003, 28, 169-178.
- [21] Leonov S.B., Yarantsev D.A., Napartovich A.P., Kochetov I.V., Plasma-Assisted Combustion of Gaseous Fuel in Supersonic Duct, *IEEE Transactions on Plasma Science* 2006, 34, 2514-2525.
- [22] Mintusov E., Serdyuchenko A., Choi I., et al, Mechanism of plasma assisted oxidation and ignition of ethylene-air flows by a repetitively pulsed nanosecond discharge, *Proceedings of the Combustion Institute*, 2009, 32, 3181-3188.
- [23] Zuzeev Y., Choi I., Uddi M., Adamovich I.V., Lempert W.R., Atomic Oxygen Measurements in Air and Air/Fuel Nanosecond Pulse Discharges by Two Photon Laser Induced Fluorescence, *J. Phys. D: Appl. Phys.*, 2010, 43, 124001, 12 pp.
- [24] Napartovich A.P., Kochetov I.V., Deminsky M.A., Potapkin B.V., Modeling of oxygen dissociation in gas mixture by pulse-periodic discharge, Proceeding of the V International Symposium on Theoretical and Applied Plasma Chemistry, Ivanovo State University of Chemistry and Technology, Ivanovo, Russia, 2008, 1, 262-265.
- [25] Napartovich A.P., Problems of modelling of non-thermal discharge evolution in chemically unstable gas mixtures, Report at Aerospace Thematic Workshop: Fundamentals of Aerodynamic Flow and Combustion Control by Plasmas, Les Houches, France, 2009, unpublished.
- [26] Baulch D.L., Bowman C.T., Cobos J., Cox R.A., Just Th., Kerr J.A., Pilling M.J., Stocker D., Troe J., Tsang W., Walker R.W., Warnatz J., Evaluated Kinetic Data for Combustion Modeling: Supplement II, *J. Phys. Chem. Ref. Data* 2005, 34, 757-1397.

